Polymer Testing 78 (2019) 105946

Contents lists available at ScienceDirect

Polymer Testing

journal homepage: www.elsevier.com/locate/polytest

Material Properties

Optimization of thermo-mechanical and antibacterial properties of epoxy/polyethylene glycol/MWCNTs nano-composites using response surface methodology and investigation thermal cycling fatigue

Mahdi Ashrafi[a], Ahmad Reza Ghasemi[b,*], Masood Hamadanian[a,c]

[a] Institute of Nanoscience and Nanotechnology, University of Kashan, Kashan, Iran
[b] Composite and Nanocomposite Research Laboratory, Department of Solid Mechanics, Faculty of Mechanical Engineering, University of Kashan, Kashan, Iran
[c] Department of Physical Chemistry, Faculty of Chemistry, University of Kashan, Iran

ARTICLE INFO

Keywords:
Mechanical/thermal properties
Polymeric nanocomposite
EP/PEG/MWCNTs
Thermal cycle loading
Antibacterial property

ABSTRACT

This work aimed to develop mechanical/thermal properties of polymer-based nanocomposite in aerospace applications. Hence, herein nanocomposites were prepared through the direct blending of epoxy (EP) with Polyethylene glycol (PEG) and multiwalled carbon nanotubes (MWCNTs) as filler. Weight fraction of fillers was optimized by central composite design (CCD) to get maximum tensile strength and elongation. Interestingly, cross-section scanning electron microscopy (cross-section SEM) and thermal gravimetric analysis (TGA) observations revealed that MWCNTs were well dispersed on polymer matrix and thermal stability of EP was strengthened. The optimized EP/PEG/MWCNTs nanocomposites were tested under 150 thermal cycles and results were shown elongation 24.83% and tensile strength 17.96% were decreased after 150 cycles. Also, cross-section SEM images clearly showed that the fractures have increased slightly. In addition, MWCNTs-Ag nanostructures were synthesized and EP/PEG/MWCNTs-Ag nanocomposites were prepared for investigation antibacterial activity. Energy dispersive spectroscopy (EDS) mapping images of MWCNTs-Ag were confirmed the homogeneous and efficient anchoring of silver on the MWCNTs. Results indicate that, Ag nanoparticles can be enhanced the antibacterial activity of EP/PEG/MWCNTs.

1. Introduction

The employment of polymer-based nanocomposite in aerospace applications has expressively improved because of their excellent specific features. Polymeric nanocomposite is a multi-phase material comprised of polymer matrix and reinforcing nanofiller. Combination of the reinforcing nanofillers results in nanocomposite material with synergistic mechanical properties that can't be achieved from either part alone [1,2]. The launch of any aerospace system into the low earth and geosynchronous orbits are generally costly. Due to rising fuel prices, the demand for lightweight materials in the aerospace industry has increased significantly. Therefore, during the past three decades, aerospace designers began to replace metal parts with polymeric matrix nanocomposites (PMNCs), which were innovative and attractive materials for the aerospace application [3–5]. On the other hand, degradation of thermo-mechanical properties of the PMNCs along the thermal cycling is the most important effect in space. Weaknesses mechanical properties, leads to limits applications of PMNCs in aerospace industry [6,7].

Epoxy resin is one of the most important thermosetting polymers [8,9]. It has many applications which are due to their unique properties such as: high strength and stiffness, resistance to chemicals, good dielectric behavior, low contraction during curing, corrosion and good thermal characteristics [10,11]. However, their brittleness, poor resistance to crack propagation and poor wear resistance limit their applications [12,13]. Recently, researchers have found that addition of carbon nanotubes (CNTs) can be improved significantly the mechanical, electrical and thermal properties of EP resin [14–16]. While elongation decreases by adding CNTs on EP which, to solve this problem, a softener was added to the EP resin.

Since the early nineties, CNTs have been vigorously attributed as high potential nanofiller material for polymer [17–19]. Owing to their significant mechanical, electronic and thermal properties because of graphite-like structure. These properties have been made it an ideal nanofiller in nanocomposites [20–23]. CNT can combine the tensile strength and high modulus. The tensile strength lies between 50 and

* Corresponding author.
E-mail addresses: mahdi.ashrafi68@gmail.com (M. Ashrafi), ghasemi@kashanu.ac.ir (A.R. Ghasemi), Hamadani@kashanu.ac.ir (M. Hamadanian).

https://doi.org/10.1016/j.polymertesting.2019.105946
Received 26 March 2019; Received in revised form 17 May 2019; Accepted 18 June 2019
Available online 19 June 2019
0142-9418/

100 GPa and Young modulus ranges from 50 to 1000 GPa. These properties make nanotube excellent candidate for the next generation nanocomposite [24]. Because of these properties, CNT is used as nanofiller in ceramics, metallic, and polymers [25]. It is of great interest to use of CNTs as nanofiller in simulation and experimental researches to reinforce polymers including EP, was well-established.

The polyethylene glycol (PEG), has a non-toxicity and is one of the water-soluble polymers. PEG with low molecular weight added in different polymer as a softener and it causes an increase the elongation [26,27]. Silver has the highest antibacterial activities and CNTs have high aspect ratio, high surface area, high mechanical strength, and high thermal and electrical conductivities with a low coefficient of thermal expansion [28–30]. Therefore, the integration of CNTs with silver is expected to produce nanocomposites with advantage of both. The main novelty of this work is determined to achieve the best mechanical properties by simultaneous adding MWCNTs as a nanofiller and PEG as a softener.

In this research, the effects of MWCNTs as nanofiller and PEG as softener were simultaneously evaluated on the tensile strength and elongation of the EP/PEG/MWCNTs nanocomposites. The central composite design (CCD) combined with response surface methodology (RSM) was applied to optimize the tensile strength and elongation EP/PEG/MWCNTs nanocomposite using two different levels of PEG and MWCNTs (wt%). Also, the optimized samples were examined under thermal cycles fatigue during different times of the cycle (50, 100 and 150 thermal cycle fatigue) and were investigated by cross-section SEM, EDS, TGA and x-ray diffraction (XRD). Finally, silver nanoparticles were deposited on the surface of the MWCNTs to improve the antibacterial properties of the nanocomposite, and the antibacterial activity of the EP/PEG/MWCNTs-Ag nanocomposite was evaluated and identified with XRD, SEM and EDS map analyses.

2. Materials and methods

2.1. Materials and characterization

Epoxy resin (KER 828) from KUMHO P&B chemical company (Korea), PEG-200 purchased from LOTTE chemical company and epoxy hardener from KUKDO chemical company are provided. $AgNO_3$, hydrazine received from Merck company and Industrial multi-walled carbon nanotubes, grade of KNT-MP (with diameter ~ 9.5 nm, length ~1.5 μm, carbon purity > 90% and BET surface area = 250–300 m2/g) were prepared from Grafen Chemical Industries.

Tensile tests of nanocomposites were carried out by a 20 kN universal testing machine model TB1The TGA curves of samples were performed through the utilization of thermal gravimetric analysis (TG-DTA, BAHR STA 503 model, Germany). XRD patterns of samples were recorded by a Philips-X'pertpro, X-ray diffractometer using Ni-filtered Cu Kα radiation. The cross-section and surface SEM images were exposed using a scanning electron microscopy (SEM, model S-4160, Hitachi, Japan) equipped with energy-dispersive spectroscopy (EDS) analysis (Peronis 2100, Japan). The EDS mapping images of MWCNTs-Ag were performed by Energy-dispersive X-ray spectroscopy (EDX) (FE-SEMs model MIRA III, France).

2.2. Preparation of EP/PEG/MWCNTs nanocomposite, MWCNTs-Ag and EP/PEG/MWCNTs-Ag nanocomposite

EP/PEG/MWCNTs nanocomposites containing different fraction of MWCNTs and PEG (wt%) listed in Table 1 were prepared via direct blending (mechanical mixing) method.

Desired amount of MWCNTs powder and PEG were poured into EP and stirred at room temperature for 1 h with the aid of a magnetic stirrer, and then sonicated for 30 min. Afterward, hardener was added to the homogenous blend and stirring for another 5 min at room temperature. The prepared blends were then poured into a silicone mold and were allowed to dry at room temperature for 24 h.

Table 1
Experimental range of independent variables and experimental design with actual response.

Variable	Level code		
	-α	0	+α
A: PEG (wt%)	5	6.5	8
B: MWCNTs (wt%)	0.1	0.3	0.5

Runs	Experimental variables		Response	
	PEG (wt%)	MWCNTs (wt%)	Tensile strength (MPa)	Elongation (%)
1	7.32	4.27	31.59	5.665
2	25.00	2.50	32.26	6.62
3	42.68	0.73	29.2	5.17
4	25.00	2.50	30.67	4.62
5	25.00	2.50	28.55	4.81
6	25.00	5.00	26.12	5.79
7	0.00	2.50	34.43	5.705
8	42.68	4.27	30.46	6.46
9	7.32	0.73	28.55	5.05
10	25.00	2.50	30.17	4.7
11	25.00	2.50	25.72	5.84
12	25.00	0.00	29.53	5.95
13	50.00	2.50	26.17	5.845

The synthesis of MWCNTs-Ag involved two steps. Firstly, surface of the MWCNTs were functionalized, as described in the earlier literature [31]. For this, 50 mg of MWCNTs were dispersed into a solution of sulfuric and nitric acids (with volume ratio 3:1) and stirred for 24 h. The solution was filtered and washed with de-ionized water several times and then was dried in a vacuum oven at 40 °C. Secondly, the functionalized MWCNTs powder were dispersed in deionized water using an ultrasonic probe sonicator at high frequency. $AgNO_3$ was added to the MWCNTs suspension (with ratio 0.5:1, 1:1, 1.5:1 and 2:1 wt%) and the solution was vigorously stirred continuously for 12 h. Minimum amount of hydrazine hydrate was added to this solution which caused a change in the color of the solution from black to light brown confirming the synthesis of MWCNTs-Ag nanostructure.

EP/PEG/MWCNTs-Ag nanocomposites were prepared with the same procedure EP/PEG/MWCNTs nanocomposites.

3. Design of experiment

Response surface methodology (RSM) is a collection of statistical and mathematical techniques useful to solve multivariate or regression equations simultaneously by using the measurement data obtained from the experimental design study [32,33]. Central composite design (CCD) is subset of RSM which is able to model and optimize related operational factors of the mechanical properties of nanocomposites and can specify the possible interaction between them [34,35]. Combined influence of PEG (wt%) and MWCNTs (wt%) (independent variables) on the tensile strength and elongation of EP (response) were evaluated. The range of two independent variables with experimental design and corresponding response are listed in Table 1.

4. Result and discussion

4.1. Statistical analysis

Based on the experimental results in Table 1, the data were analyzed by the design expert software. The analysis of variance (ANOVA) table was used to evaluate the explanatory power of each variable [36]. The ANOVA for tensile strength and elongation were summarized in Tables

Table 2
ANOVA for tensile strength of EP/PEG/MWCNTs nanocomposites.

Source	Sum of Squares	df	Mean Square	F Value	p-value Prob > F	
Model	71.72	2	35.86	60.43	< 0.0001	significant
A-PEG	41.93	1	41.93	70.67	< 0.0001	
B-CNT	29.78	1	29.78	50.19	< 0.0001	
Residual	5.93	10	0.59			
Lack of Fit	2.24	6	0.37	0.40	0.8457	not significant
Pure Error	3.69	4	0.92			
Cor Total	77.65	12				

Table 3
ANOVA for elongation of EP/PEG/MWCNTs nanocomposite.

Source	Sum of Squares	df	Mean Square	F Value	p-value Prob > F	
Model	4.61	5	0.92	20.41	0.0005	significant
A-PEG	0.30	1	0.30	6.63	0.0367	
B-CNT	0.10	1	0.10	2.24	0.1783	
AB	0.19	1	0.19	4.14	0.0814	
A^2	3.12	1	3.12	69.03	< 0.0001	
B^2	1.38	1	1.38	30.44	0.0009	
Residual	0.32	7	0.045			
Lack of Fit	0.099	3	0.033	0.61	0.6447	not significant
Pure Error	0.22	4	0.054			
Cor Total	4.93	12				

2 and 3, respectively. The model "F value" of 60.43 and 20.41 suggested the model of tensile strength and elongation were significant. The "lack of fit F value" of 0.40 and 0.61 implied the "lack of fit" of these models were not significant relative to pure error. Additionally, the "R-squared" of 0.9236 and 0.9358 of tensile strength and elongation was in reasonable agreement with the "Adj R-square" of 0.9083 and 0.8899, which suggested the model fits well. The empirical relationships between the response variable and independent variables were described as follows:

Tensile strength: $Y = +29.49 - 2.29 \times A + 1.93 \times B$ (1)

Elongation: $Y = +4.87 - 0.19 \times A - 0.11 \times B + 0.22 \times AB + 0.67A^2 + 0.44 \times B^2$ (2)

Where, Y is the response, A corresponds to PEG (wt%) and B corresponds to MWCNTs (wt%).

In order to have a better understanding of the relationship between the independent variables and the effect of their interactions on tensile strength and elongation, the three-dimensional (3D) response surface plots were used and presented in Fig. 1. The effect of MWCNTs and PEG (wt%) by Eq. (1) using the tensile strength is shown in Fig. 1a. It clearly shows that tensile strength considerably increased with increasing the amount of MWCNTs from 0.1 to 0.5 (wt%) when the amount of PEG was low, while slightly decreased with increasing the amount of PEG from 5.00 to 8.00 wt% when the amount of MWCNTs was low.

The effect of MWCNTs and PEG (wt%) on elongation is shown in Fig. 1b. Both factors show the same tendency, where the elongation first decreased, then increased with increasing MWCNTs and PEG (wt%). This plot was in agreement with the ANOVA results, where the quadratic terms (Eq. (2)) for MWCNTs and PEG were shown to be significant and to have positive effects on the elongation.

4.2. Thermal cycle loading fatigue

For optimization purposes, the desired goal for tensile strength and elongation was chosen to a maximum, along with two independent variables to be within range. Under the optimized condition tensile strength and elongation 37.156 (MPa) and 3.632 (%) were obtained, respectively. After optimization, the optimal specimen over thermal cycles test consisted of 150 thermal cycles using developed thermal cycling apparatus was investigated [37]. The temperature range of the thermal cycle was set tween 0 °C and 80 °C (rate: ~ 9 °C/min). An example of a temperature record of the test is given in Fig. 2a.

The stress-strain curves of the nanocomposite under different number of thermal cycling fatigue are provided in Fig. 2b. It has been concluded from the results of the stress-strain curves, that the number of thermal cycles has no significant effect on the Young's modulus and remains almost constant. While, with increasing number of thermal cycles elongation, tensile strength and the area under the stress–strain curve were decreased. However, this decrease is not linear, since the nature of the thermal cyclic effects on mechanical properties is not linear. Also, according to Fig. 2c elongation (15.3%, 17.51% and 24.83%) and tensile strength (8.31%, 16.49% and 17.96%) were decreased after 50, 100 and 150 thermal cycle loading, respectively.

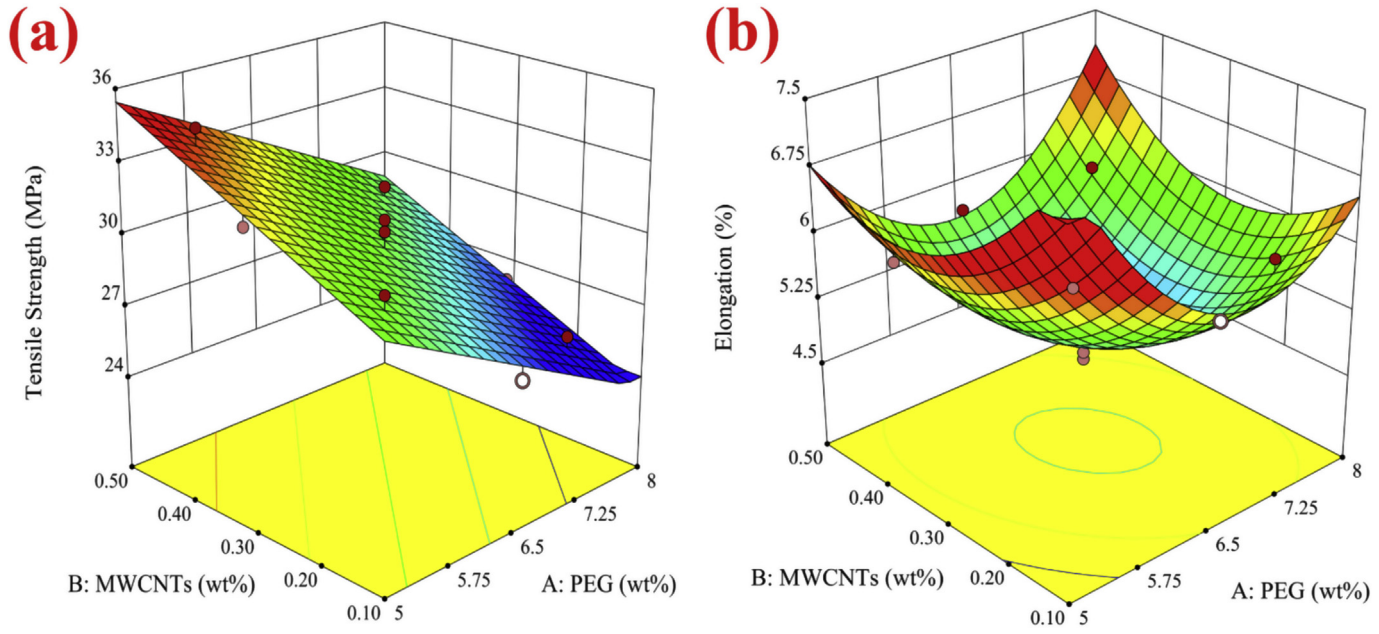

Fig. 1. 3D plot interaction of the PEG and MWCNTs (wt%) on tensile strength (a) and elongation (b).

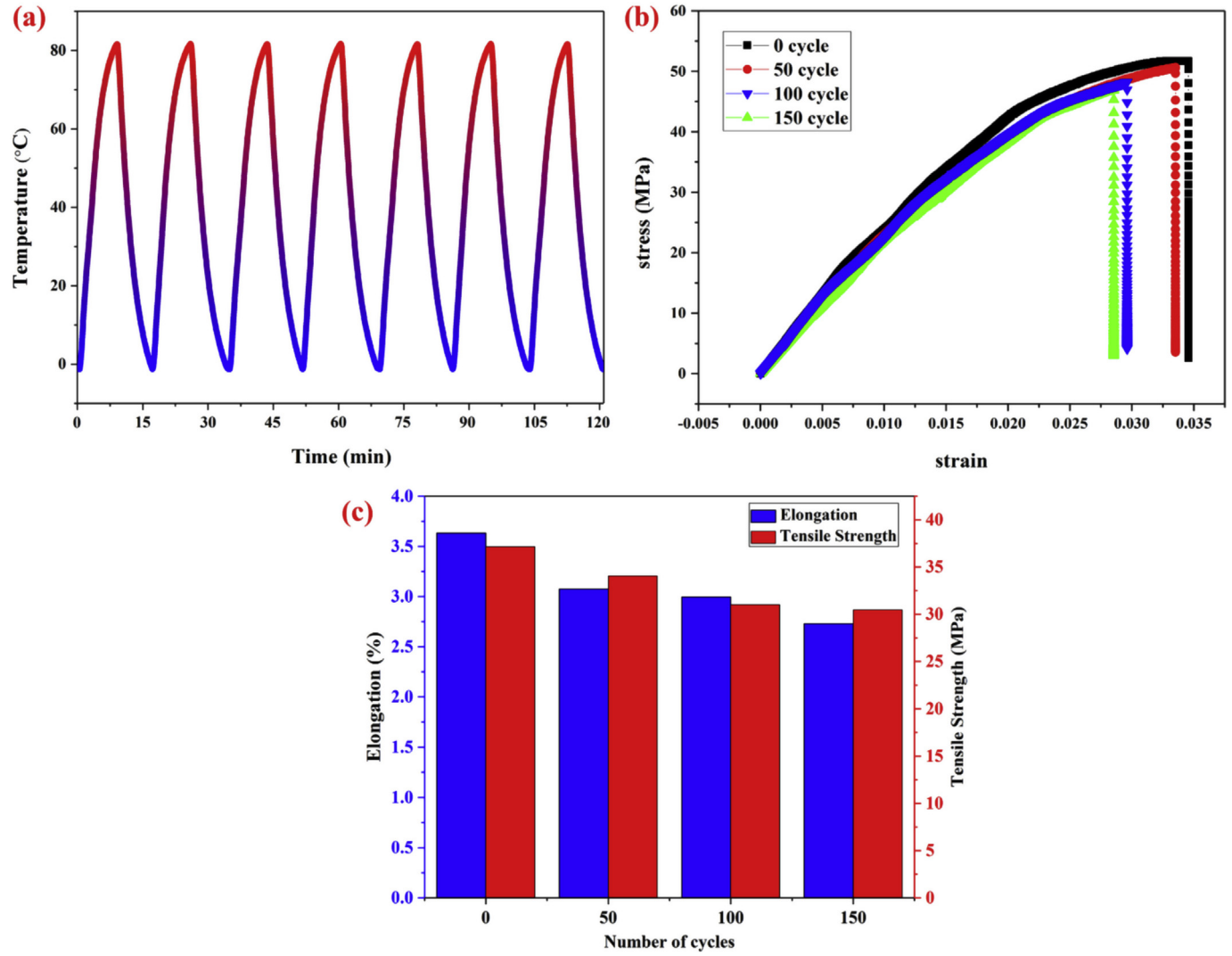

Fig. 2. An example of a temperature record of the test (a), stress-strain curves of the EP/PEG/MWCNTs nanocomposite (b) and average tensile strength and elongation after different condition of thermal cycling (c).

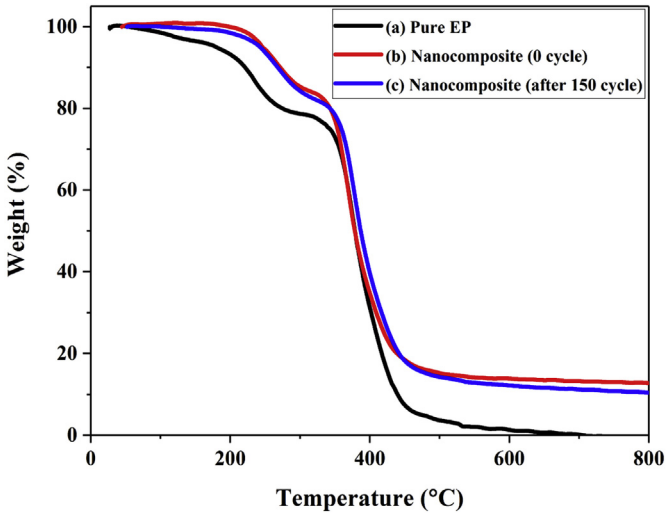

Fig. 3. TGA curves of pure EP (a), EP/PEG/MWCNTs (b) and EP/PEG/MWCNTs after 150 thermal cycling loading.

4.3. TGA analysis

TGA curves of the samples, under an argon atmosphere at a heating rate of 10 K min^{-1} are summarized in Fig. 3. The TGA curves of all samples have two thermal degradation stages: in the first stage, samples were burnt and in the second stage, the char layer formed at high temperature were degraded further [38,39]. Pure EP decomposition at almost 810 °C, while EP/PEG/MWCNTs samples were not completely degraded at the same temperature. It clearly shows that, thermal stability of pure EP by blending MWCNTs and PEG were increased. TGA curve of EP/PEG/MWCNTs after 150-cycle a similar the initial EP/PEG/MWCNTs, that it was shown that the thermal cycling has no effect on the thermal stability of the nanocomposite.

4.4. XRD analysis

Fig. 4 shows the XRD patterns of EP/PEG, EP/PEG/MWCNTs, MWCNTs/Ag and EP/PEG/(MWCNTs/Ag). It can be seen from Fig. 4a that a wide diffraction was appeared in the XRD pattern of the EP/PEG from 5 to 30° which is caused by scattering of the cured EP molecules, revealing its amorphous nature. The diffractogram of EP/PEG/MWCNTs nanocomposite is very similar to that of the neat EP/PEG and a slight shifting in peak position at 2θ values was observed. The presence of characteristic peaks along with shifting of 2θ positions

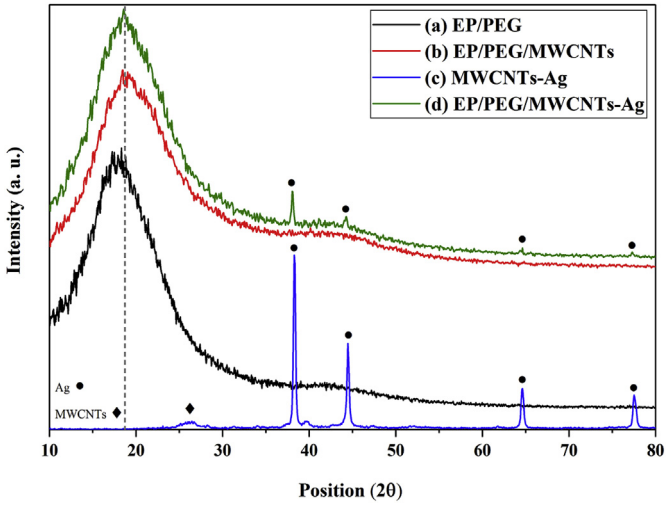

Fig. 4. XRD pattern of EP/PEG (a), EP/PEG/MWCNTs (b), MWCNTs-Ag (c) and EP/PEG/MWCNTs-Ag.

indicates better intercalation of MWCNTs by the EP matrix and gives the evidence of the formation of EP/PEG/MWCNTs nanocomposites (Fig. 4b) [40]. Diffraction peaks at 38.3°, 44.5°, 64.57° and 77.48° can be attributed to (111), (200), (220) & (311) reflections of cubic phase of silver (JCPDS card No. 003–0921) and MWCNTs presence in the sample are indicated by slight bulge at 22.46° (Fig. 4c) [41]. The XRD pattern of EP/PEG/MWCNTs-Ag (1:2 wt%) nanocomposite showed lower intensity diffraction peaks than MWCNTs-Ag, which is due to its low amount of MWCNTs-Ag (Fig. 4d).

4.5. SEM and EDS analysis

A high-resolution SEM image of a selected area in the cross section reveals MWCNTs were well randomly dispersed and mixed throughout the polymer matrix. According to the SEM images (Fig. 5a–h), clearly show that the ratio of fractures and defects slightly increased. Since the mechanical properties will be dependent upon the presence of defects [42], which with increasing number of thermal cycles, both the tensile strength and elongation at break were decreased.

SEM images and EDS spectra of MWCNTs-Ag and EP/PEG/MWCNTs-Ag are shown in Fig. 6 a-d. As can be observed in Fig. 6a, the Ag nanoparticles show a high degree of agglomeration and MWCNTs are densely entangled. SEM image of EP/PEG/MWCNTs-Ag is shown that the MWCNTs-Ag nanoparticles are randomly and fine dispersed in matrix. The presence of silver, carbon, oxygen and nitrogen content can be confirmed by EDS spectra (Fig. 6c and d). By comparing Fig. 6 c with Fig. 6d carbon and oxygen content increased and nitrogen was appeared but silver content decreased, which are due to the polymer matrix composites.

EDS mapping images of MWCNTs-Ag hybrid samples for C, O and Ag elements in the selected area evidently confirmed the homogeneous and efficient anchoring of silver on the MWCNTs (Fig. 6e).

4.6. Antibacterial activity

The antibacterial activity of samples was determined via disk diffusion method against gram-negative *Escherichia coli* (*E. coli*, ATCC 9637). In disc diffusion method, the samples were catted into round discs (6 mm in diameter) and subjected to the nutrient agar plates consisted of bacteria cells and then the plates were incubated at 37 °C for 24 h. The silver free film and gentamicin antibiotic disc (Padtan Teb, Iran) were placed on the plates as the negative and positive control discs, respectively. The zone of the inhibition (ZOI) around the discs were measured to determine the relative antibacterial effect of the samples [43,44].

The antibacterial activity of pure EP, EP/PEG/MWCNTs and EP/PEG/MWCNTs-Ag nanocomposite with different concentrations of Ag have been displayed in Fig. 7. According to Fig. 7a, it can be clearly

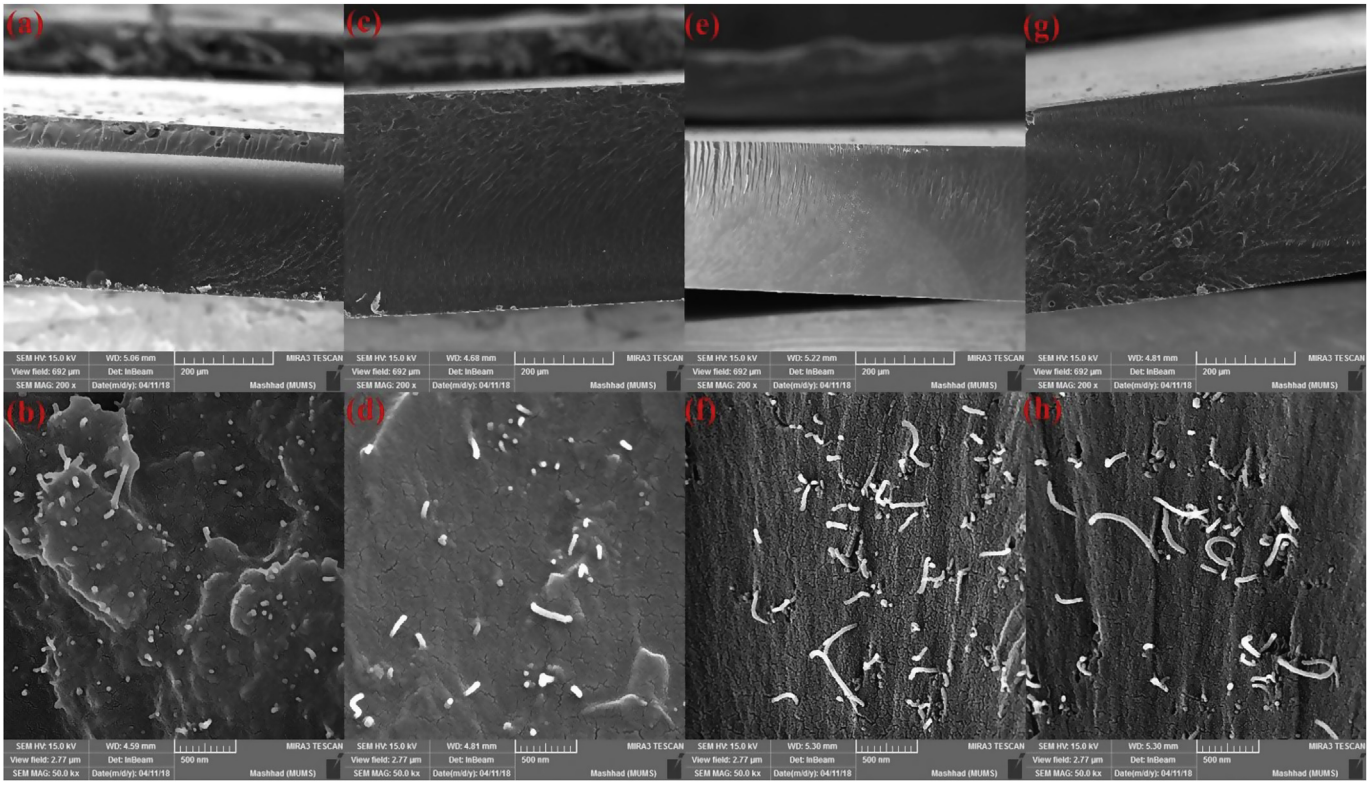

Fig. 5. Cross-section SEM images of EP/PEG/MWCNTs after 0 cycle (a and b), 50 cycle (c and d), 100 cycle (e and f) and 150 thermal cycle loading.

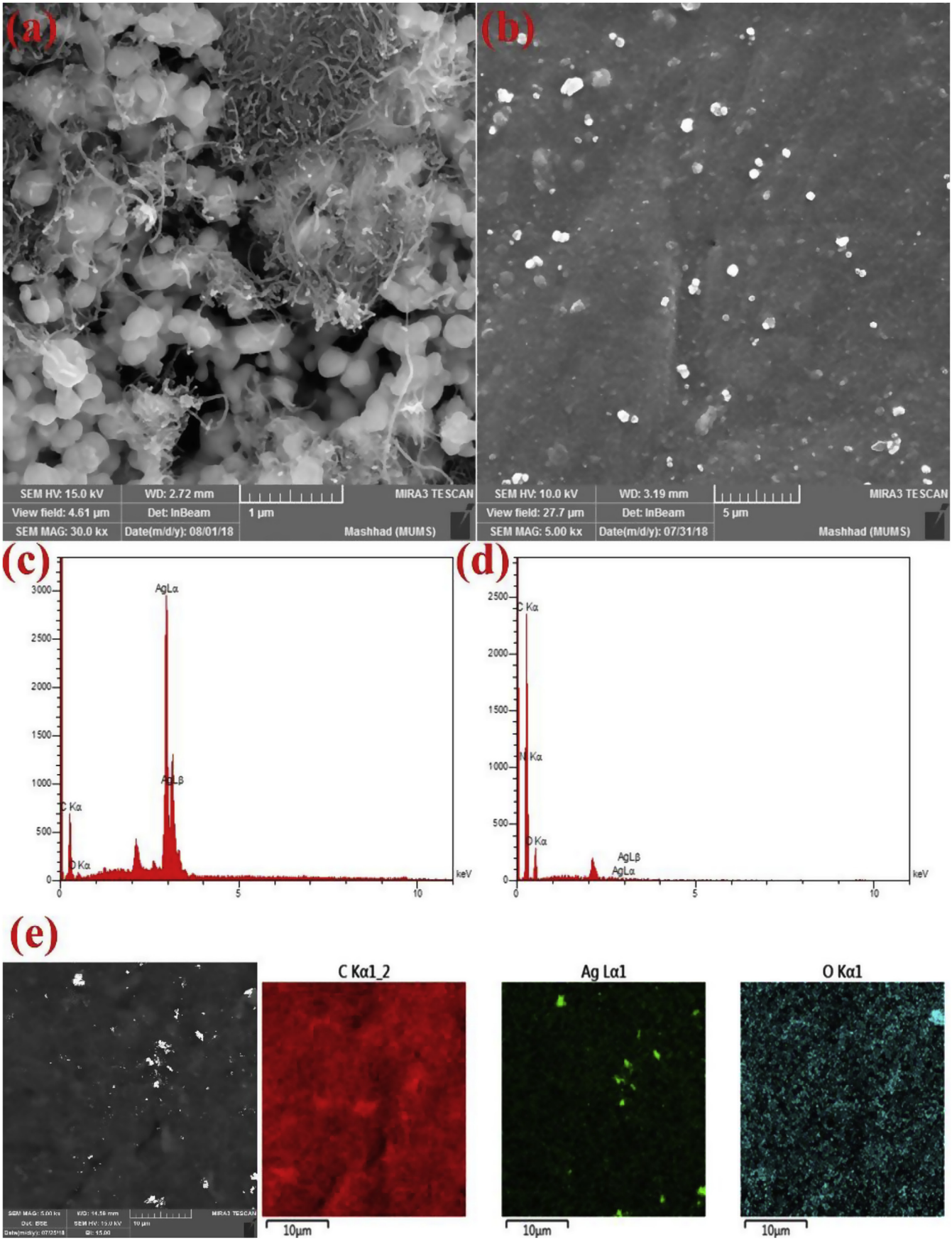

Fig. 6. SEM image of MWCNTs-Ag (1:2 wt%) (a), surface SEM image of EP/PEG/MWCNTs-Ag (1:2 wt%) (b), EDS spectra of MWCNTs-Ag (c), EDS spectra of EP/PEG/MWCNTs-Ag (d) and EDS mapping images of MWCNTs-Ag (e).

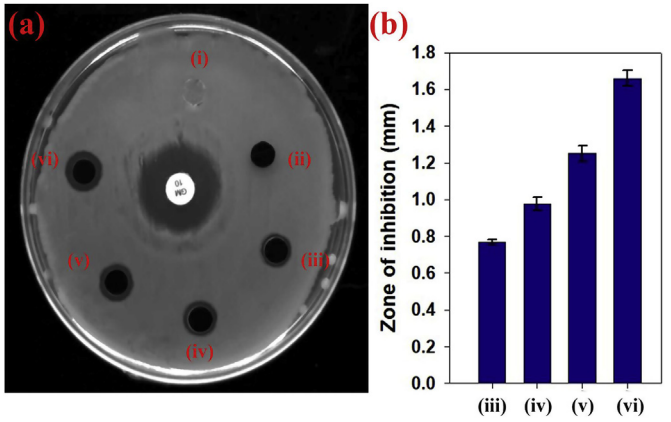

Fig. 7. The antibacterial activity evaluation of pure EP (i), EP/PEG/MWCNTs (ii), EP/PEG/MWCNTs-Ag (1:0.5 wt%) (iii), EP/PEG/MWCNTs-Ag (1:1 wt%) (iv), EP/PEG/MWCNTs-Ag (1:1.5 wt%) (v), EP/PEG/MWCNTs-Ag (1:2 wt%) (vi) via disk diffusion method against *E. coli* (a) and zone of inhibition of samples containing Ag nanoparticle (b).

seen that EP/PEG and EP/PEG/MWCNTs have no influence on the growth of bacterial. However, a clear ZOI around the samples containing Ag nanoparticles can be observed, which has increased with increasing concentrations of Ag (w/w %) (Fig. 7b). The results indicated that the EP/PEG/MWCNTs nanocomposites containing Ag nanoparticles held antibacterial property for the presence of silver nanoparticles.

5. Conclusions

In this research, EP/PEG/MWCNTs nanocomposites were prepared through the direct blending method and weight fractions of PEG and MWCNTs (wt%) were optimized by CCD to get maximum the tensile strength and elongation. The silver nanoparticles were deposited on the surface of the MWCNTs to improve the antibacterial properties of the nanocomposite aganist *E. coli*. The ZOI around the samples containing Ag nanoparticles can be observed, which have increased with increasing concentrations of Ag (wt%).

Cross-section SEM images were showed that with increasing number of thermal cycling, fractures on the nanocomposite matrix were increased, therefore the tensile strength and elongation of nanocomposite were decreased. The results obtained of stress-strain curves were found that the tensile strength (8.31%, 16.49% and 17.96%) and elongation (15.3%, 17.51% and 24.83%) were decreased after 50, 100 and 150 thermal cycles, respectively, while TGA analysis confirmed that the thermal stability of EP was remarkably improved in the presence of MWCNT and it has not changed during thermal cycling.

References

[1] J. Njuguna, K. Pielichowski, Polymer nanocomposites for aerospace applications: fabrication, Adv. Eng. Mater. 6 (4) (2004) 193–203.
[2] V.T. Rathod, J.S. Kumar, A. Jain, Polymer and ceramic nanocomposites for aerospace applications, Appl. Nanosci. 7 (8) (2017) 519–548.
[3] J. Njuguna, K. Pielichowski, J. Fan, Polymer nanocomposites for aerospace applications, Advances in Polymer Nanocomposites, Elsevier, 2012, pp. 472–539.
[4] A.D. Kelkar, Q. Tian, D. Yu, L. Zhang, Boron nitride nanoparticle enhanced prepregs: a novel route for manufacturing aerospace structural composite laminate, Mater. Chem. Phys. 176 (2016) 136–142.
[5] M.K. Pitchan, S. Bhowmik, M. Balachandran, M. Abraham, Process optimization of functionalized MWCNT/polyetherimide nanocomposites for aerospace application, Mater. Des. 127 (2017) 193–203.
[6] J.M. Sousa, J.R. Correia, S. Cabral-Fonseca, A.C. Diogo, Effects of thermal cycles on the mechanical response of pultruded GFRP profiles used in civil engineering applications, Compos. Struct. 116 (2014) 720–731.
[7] N. Hancox, Thermal effects on polymer matrix composites: Part 1. Thermal cycling, Mater. Des. 19 (3) (1998) 85–91.
[8] O. Castro, P.A. Carraro, L. Maragoni, M. Quaresimin, Fatigue damage evolution in unidirectional glass/epoxy composites under a cyclic load, Polym. Test. 74 (2019) 216–224.
[9] K. Huang, Z. Liu, J. Zhang, S. Li, M. Li, J. Xia, et al., A self-crosslinking thermosetting monomer with both epoxy and anhydride groups derived from tung oil fatty acids: synthesis and properties, Eur. Polym. J. 70 (2015) 45–54.
[10] Z. Heng, Y. Chen, H. Zou, M. Liang, Simultaneously enhanced tensile strength and fracture toughness of epoxy resins by a poly (ethylene oxide)-block-carboxyl terminated butadiene-acrylonitrile rubber dilock copolymer, RSC Adv. 5 (53) (2015) 42362–42368.
[11] T. Wu, Y. Liu, N. Li, G.-W. Huang, C.-B. Qu, H.-M. Xiao, Cryogenic mechanical properties of epoxy resin toughened by hydroxyl-terminated polyurethane, Polym. Test. 74 (2019) 45–56.
[12] J. Parameswaranpillai, S. Krishnan Sidhardhan, S. Jose, S. Siengchin, J. Pionteck, A. Magueresse, et al., Reaction-induced phase separation and resulting thermo-mechanical and surface properties of epoxy resin/poly (ethylene oxide)–poly (propylene oxide)–poly (ethylene oxide) blends cured with 4, 4′-diaminodiphenylsulfone, J. Appl. Polym. Sci. 134 (4) (2017).
[13] C. Monteserín, M. Blanco, E. Aranzabe, A. Aranzabe, J.M. Laza, A. Larrañaga-Varga, et al., Effects of graphene oxide and chemically-reduced graphene oxide on the dynamic mechanical properties of epoxy amine composites, Polymers 9 (9) (2017) 449.
[14] A. Kausar, I. Rafique, B. Muhammad, Review of applications of polymer/carbon nanotubes and epoxy/CNT composites, Polym. Plast. Technol. Eng. 55 (11) (2016) 1167–1191.
[15] N. Domun, H. Hadavinia, T. Zhang, T. Sainsbury, G. Liaghat, S. Vahid, Improving the fracture toughness and the strength of epoxy using nanomaterials–a review of the current status, Nanoscale 7 (23) (2015) 10294–10329.
[16] B. Saboori, M.R. Ayatollahi, Experimental fracture study of MWCNT/epoxy nanocomposites under the combined out-of-plane shear and tensile loading, Polym. Test. 59 (2017) 193–202.
[17] R.K. Prusty, D.K. Rathore, B.C. Ray, CNT/polymer interface in polymeric composites and its sensitivity study at different environments, Adv. Colloid Interface Sci. 240 (2017) 77–106.
[18] X. Sun, H. Sun, H. Li, H. Peng, Developing polymer composite materials: carbon nanotubes or graphene? Adv. Mater. 25 (37) (2013) 5153–5176.
[19] M.H. Al-Saleh, Clay/carbon nanotube hybrid mixture to reduce the electrical percolation threshold of polymer nanocomposites, Compos. Sci. Technol. 149 (2017) 34–40.
[20] H. Gu, J. Guo, H. Wei, S. Guo, J. Liu, Y. Huang, et al., Strengthened magnetoresistive epoxy nanocomposite papers derived from synergistic nanomagnetite--carbon nanofiber nanohybrids, Adv. Mater. 27 (40) (2015) 6277–6282.
[21] L. Yue, G. Pircheraghi, S.A. Monemian, I. Manas-Zloczower, Epoxy composites with carbon nanotubes and graphene nanoplatelets–Dispersion and synergy effects, Carbon 78 (2014) 268–278.
[22] T.H. Nam, K. Goto, Y. Yamaguchi, E. Premalal, Y. Shimamura, Y. Inoue, et al., Improving mechanical properties of high volume fraction aligned multi-walled carbon nanotube/epoxy composites by stretching and pressing, Composites Part B 85 (2016) 15–23.
[23] L. Rodríguez-Pérez, C. Villegas, MAn Herranz, J.L. Delgado, N. Martín, Heptamethine cyanine dyes in the design of photoactive carbon nanomaterials, ACS Omega 2 (12) (2017) 9164–9170.
[24] I. Rafique, A. Kausar, Z. Anwar, B. Muhammad, Exploration of epoxy resins, hardening systems, and epoxy/carbon nanotube composite designed for high performance materials: a review, Polym. Plast. Technol. Eng. 55 (3) (2016) 312–333.
[25] F.-C. Chiu, Y.-C. Chuang, S.-J. Liao, Y.-H. Chang, Comparison of PVDF/PVAc/GNP and PVDF/PVAc/CNT ternary nanocomposites: enhanced thermal/electrical properties and rigidity, Polym. Test. 65 (2018) 197–205.
[26] B.W. Chieng, N.A. Ibrahim, W.M.Z.W. Yunus, M.Z. Hussein, Poly (lactic acid)/poly (ethylene glycol) polymer nanocomposites: effects of graphene nanoplatelets, Polymers 6 (1) (2013) 93–104.
[27] C. Zhang, M.R. Salick, T.M. Cordie, T. Ellingham, Y. Dan, L.-S. Turng, Incorporation of poly (ethylene glycol) grafted cellulose nanocrystals in poly (lactic acid) electrospun nanocomposite fibers as potential scaffolds for bone tissue engineering, Mater. Sci. Eng. C 49 (2015) 463–471.
[28] J. López-Esparza, LnF. Espinosa-Cristóbal, A. Donohue-Cornejo, SnY. Reyes-López, Antimicrobial activity of silver nanoparticles in polycaprolactone nanofibers against gram-positive and gram-negative bacteria, Ind. Eng. Chem. Res. 55 (49) (2016) 12532–12538.
[29] S. Begum, H. Ullah, A. Kausar, M. Siddiq, M.A. Aleem, Fabrication of epoxy functionalized MWCNTs reinforced PVDF nanocomposites with high dielectric permittivity, low dielectric loss and high electrical conductivity, Compos. Sci. Technol. 167 (2018) 497–506.
[30] M. Elias, M.K. Amin, S.H. Firoz, M.A. Hossain, S. Akter, M.A. Hossain, et al., Microwave-assisted synthesis of Ce-doped ZnO/CNT composite with enhanced photo-catalytic activity, Ceram. Int. 43 (1) (2017) 84–91.
[31] S. Wang, Q. Lin, J. Chen, H. Gao, D. Fu, S. Shen, Biocompatible polydopamine-encapsulated gadolinium-loaded carbon nanotubes for MRI and color mapping guided photothermal dissection of tumor metastasis, Carbon 112 (2017) 53–62.
[32] A. Dean, D. Voss, D. Draguljić, Response Surface Methodology. Design and Analysis of Experiments, Springer, 2017, pp. 565–614.
[33] S.R. Mirmasoomi, M.M. Ghazi, M. Galedari, Photocatalytic degradation of diazinon under visible light using TiO_2/Fe_2O_3 nanocomposite synthesized by ultrasonic-assisted impregnation method, Separ. Purif. Technol. 175 (2017) 418–427.
[34] M. Zbair, Z. Anfar, H.A. Ahsaine, N. El Alem, M. Ezahri, Acridine orange adsorption by zinc oxide/almond shell activated carbon composite: operational factors, mechanism and performance optimization using central composite design and surface

modeling, J. Environ. Manag. 206 (2018) 383–397.
[35] F. Nemati, R. Zare-Dorabei, M. Hosseini, M.R. Ganjali, Fluorescence turn-on sensing of thiamine based on Arginine–functionalized graphene quantum dots (Arg-GQDs): central composite design for process optimization, Sensor. Actuator. B Chem. 255 (2018) 2078–2085.
[36] L. Yao, X. Wang, H. Liu, C. Lin, L. Pang, J. Yang, et al., Optimization of ultrasound-assisted magnetic retrieval-linked ionic liquid dispersive liquid–liquid micro-extraction for the determination of cadmium and lead in water samples by graphite furnace atomic absorption spectrometry, J. Ind. Eng. Chem. 56 (2017) 321–326.
[37] A. Ghasemi, M. Moradi, Effect of thermal cycling and open-hole size on mechanical properties of polymer matrix composites, Polym. Test. 59 (2017) 20–28.
[38] K. Pender, L. Yang, Investigation of the potential for catalysed thermal recycling in glass fibre reinforced polymer composites by using metal oxides, Composer Part A Appl Sci Manuf 100 (2017) 285–293.
[39] T. Qu, N. Yang, J. Hou, G. Li, Y. Yao, Q. Zhang, et al., Flame retarding epoxy composites with poly (phosphazene-co-bisphenol A)-coated boron nitride to improve thermal conductivity and thermal stability, RSC Adv. 7 (10) (2017) 6140–6151.
[40] S. Gantayat, N. Sarkar, G. Prusty, D. Rout, S.K. Swain, Designing of epoxy matrix by chemically modified multiwalled carbon nanotubes, Adv. Polym. Technol. 37 (1) (2018) 176–184.
[41] G. Jia, Y. Hu, Q. Qian, Y. Yao, S. Zhang, Z. Li, et al., Formation of hierarchical structure composed of (Co/Ni) Mn-LDH nanosheets on MWCNT backbones for efficient electrocatalytic water oxidation, ACS Appl. Mater. Interfaces 8 (23) (2016) 14527–14534.
[42] B.A. Newcomb, L.A. Giannuzzi, K.M. Lyons, P.V. Gulgunje, K. Gupta, Y. Liu, et al., High resolution transmission electron microscopy study on polyacrylonitrile/carbon nanotube based carbon fibers and the effect of structure development on the thermal and electrical conductivities, Carbon 93 (2015) 502–514.
[43] A.R. Unnithan, A.G. Nejad, A.R.K. Sasikala, R.G. Thomas, Y.Y. Jeong, P. Murugesan, et al., Electrospun zwitterionic nanofibers with in situ decelerated epithelialization property for non-adherent and easy removable wound dressing application, Chem. Eng. J. 287 (2016) 640–648.
[44] Z. Hadisi, J. Nourmohammadi, S.M. Nassiri, The antibacterial and anti-inflammatory investigation of Lawsonia Inermis-gelatin-starch nano-fibrous dressing in burn wound, Int. J. Biol. Macromol. 107 (2018) 2008–2019.